

Heavy Element Enrichment of the Gas Giant Planets

by

Jaime Lee Coffey

Hon.B.Sc., The University of Toronto, 2006

A THESIS SUBMITTED IN PARTIAL FULFILMENT OF
THE REQUIREMENTS FOR THE DEGREE OF

Master of Science

in

The Faculty of Graduate Studies

(Astronomy)

The University Of British Columbia
Vancouver, Canada

August 2008

© Jaime Lee Coffey 2008

Abstract

According to both spectroscopic measurements and interior models, Jupiter, Saturn, Uranus and Neptune possess gaseous envelopes that are enriched in heavy elements compared to the Sun. Straightforward application of the dominant theories of gas giant formation - core accretion and gravitational instability - fail to provide the observed enrichment, suggesting that the surplus heavy elements were somehow dumped onto the planets after the envelopes were already in existence.

Previous work has shown that if giant planets rapidly reached their current configuration and radii, they do not accrete the remaining planetesimals efficiently enough to explain their observed heavy-element surplus. We explore the likely scenario that the effective accretion cross-sections of the giants were enhanced by the presence of the massive circumplanetary disks out of which their regular satellite systems formed. Perhaps surprisingly, we find that a simple model with protosatellite disks around Jupiter and Saturn can meet known constraints without tuning any parameters. Furthermore, we show that the heavy-element budgets in Jupiter and Saturn can be matched slightly better if Saturn's envelope (and disk) are formed roughly 0.1 – 10 Myr after that of Jupiter.

We also show that giant planets forming in an initially-compact configuration can acquire the observed enrichments if they are surrounded by similar protosatellite disks.

Protosatellite disks efficiently increase the capture cross-section, and thus the metallicity, of the giant planets. Detailed models of planet formation must therefore account for the presence of such disks during the early stages of solar system formation.

Table of Contents

Abstract	ii
Table of Contents	iii
List of Tables	v
List of Figures	vi
Acknowledgements	vii
1 Scientific Background	1
1.1 The Structure of the Giant Planets	1
1.2 Planet Formation	2
1.2.1 Core Accretion	2
1.2.2 Gravitational Instability	3
1.3 Giant Planet Composition	4
1.3.1 Heavy Element Abundances from Observations	4
1.3.2 Envelope Enrichment from Structure Studies	5
1.3.3 Solar Composition	7
1.4 Dynamical Models of Solar System Clearing	7
2 Methods	10
2.0.1 Solar System Model	10
2.0.2 SWIFT RMVS3 Symplectic Integrator	13
2.0.3 Experimental Hardware	14
3 Results	15
3.1 Baseline case	15
3.2 Protosatellite Disks	16
3.2.1 A simple protosatellite disk model	16
3.2.2 Simultaneous formation of Jupiter and Saturn	18
3.2.3 Evolution of Uranus and Neptune	23

Table of Contents

3.2.4	Delayed formation of Saturn	23
3.2.5	Mass transfer to the outer Solar System	24
3.2.6	Compact Configuration	27
4	Conclusions	30
	Bibliography	32
 Appendices		
A	Consistency and Accuracy Tests	35
A.1	Core Mass	35
A.2	Eccentricity	35
A.3	Close Encounter Log and Integration Step Size	36
A.4	Inclination distribution	37
B	Notes on Publication	41

List of Tables

1.1	Giant Planet Orbital and Physical Parameters	1
A.1	Accumulated Metals for $e_0=0$ and $e_0 =0.1$	36

List of Figures

1.1	Jupiter and Saturn Abundance Comparison to Solar	5
2.1	Depiction of the heavy-element distribution in the protoplanetary disk.	12
3.1	Heavy Element Accumulation in Baseline Case	17
3.2	Comparison of Minimum Planetesimal Diameter	19
3.3	Heavy Element Accumulation Efficiencies as a Function of a_0	21
3.4	Planetary Heavy-Element Enrichment as a Function of Pro-tosatellite Disk Lifetime	22
3.5	Comparison of Results to Theory	25
3.6	Mass Transfer to the Outer Solar System	28
A.1	Planetesimal orbital instability time scale between $10 M_{\oplus}$ cores	38
A.2	Jupiter Close Encounters - Calculated vs Logged Pericenter .	39
A.3	Jupiter Close Encounters - Inclination Distribution	40

Acknowledgements

This work would not have been possible without the guidance and help of Dr. Brett Gladman. I owe a debt of gratitude to Dr. Gladman for his unwavering support and guidance. I am also thankful for the numerous opportunities he provided me with to explore and develop my interest in all areas of planetary science.

I would also like to thank Dr. Tristan Guillot of the Observatoire de la Cote D'Azur. His patience in the face of my ignorance of the intricacies of interior modeling are greatly appreciated, as were all of his useful suggestions and insights. Finally, my thanks to Ingrid Stairs who acted as second reader for this thesis.

Chapter 1

Scientific Background

1.1 The Structure of the Giant Planets

Planets within the Solar System can be divided into two regimes: the terrestrial planets in the inner regions of the solar system, and the giant planets. The giant planets can also be subdivided into the gas and ice giants, with Jupiter and Saturn belonging to the former and Uranus and Neptune making up the latter. As suggested by this nomenclature, the outer envelopes of Jupiter and Saturn are largely composed of gases (molecular H_2), while Uranus and Neptune incorporate large amounts of ices into their structures. A more detailed discussion of the composition of the giant planets appears below in Section 1.3.

In addition to their compositions, additional physical characteristics make the divide between gas and ice giant planets a natural one. With orbital semi-major axes of 5.2 and 9.5 AU respectively, Jupiter and Saturn are in much closer proximity to the Sun than Uranus and Neptune (at 19.2 and 30.1 AU). Furthermore, the gas giants are significantly larger and more massive than their ice giant counterparts. The additional mass in turn causes the internal pressures of the gas giants to greatly exceed those expected in Uranus and Neptune. See Table 1.1 for a summary of physical characteristics.

Planet	a (AU)	mass (10^{24} kg)	Equatorial radius (km)
Jupiter	5.20336301	1898.6	71492±4
Saturn	9.53707032	568.46	60268±4
Uranus	19.19126393	86.832	25559±4
Neptune	30.06896348	102.43	24766±15

Table 1.1: The quantities in the above table illustrate the natural division between the larger, more massive gas giants and the smaller ice giants. All values from Yoder (1995).

1.2 Planet Formation

The earliest stages of planet formation have been well-studied through data from both our Solar System and extra-solar systems. The studies have shown that solar system formation begins when a protostellar nebula collapses to form a young stellar object surrounded by a flat protoplanetary disk of dust and gas. Observational evidence suggests that the dust disk lifetime is ~ 6 Myr (Haisch et al., 2001), while the gas in the disk may last for up to ~ 10 Myr (Jayawardhana et al., 2006). The shorter ‘dust lifetime’ occurs because the solids are efficiently extracted from the gas and formed into the so-called planetesimals, whose emission is undetectable. This thesis is not concerned with terrestrial planet formation (which is better understood), but rather with building the giant planets. The short lifetime of disks provides a natural constraint on the timescale of giant planet formation; the gas giants in the local solar system are composed primarily of hydrogen and helium, and therefore must have formed before the gas was lost from the system (Lissauer, 1993).

The subsequent stages of planet formation are less understood. While there are many theories regarding the giant planet formation process, they can be divided into two groups. The ‘core accretion’ theories posit that successively larger particles build up solid planetary cores (see Lissauer (1993) for a discussion of the mechanisms leading to core formation). The second group of models suggests that planets are the product of a localized instability that leads to the gravitational collapse of a portion of the protoplanetary disk (Boss, 1997).

1.2.1 Core Accretion

Pollack et al. (1996) divide the formation of the gas giants through planetesimal accretion into three stages: the aggregation of solid planetesimals into a core of order 10 Earth masses (henceforth defined as M_{\oplus}), a slow accretion of solid and gaseous material, and then the build-up of an outer envelope through rapid gas accretion. The core is formed predominantly from the heavy-element rich planetesimals located in the ‘feeding zone’ of the protoplanet, an area generally taken to encompass a region of a few Hill radii¹ around the planet (Alibert et al., 2005). Much of the initial heavy element abundance has been removed from the feeding zone by the end of

¹ Defined as $a(\frac{M_{planet}}{3M_{\odot}})^{\frac{1}{3}}$, the Hill radius is the radius of the sphere (centred on the planet) over which the gravity of the planet is dominant to that of the Sun.

this stage, leaving behind the gas. The bulk of the mass is now heavily sub-solar in metallicity.

After the core has formed, there follows a prolonged period in which the protoplanet slowly accumulates both gas and dust. Once the envelope becomes sufficiently massive ($\sim 30 M_{\oplus}$), runaway gas accretion commences (Alibert et al., 2005; Pollack et al., 1996). At this stage the planets accumulate their gaseous outer layers from the metal-depleted feeding zone. A straight-forward application of this theory would thus predict that the gas giant atmospheres form with sub-solar levels of heavy elements. As is usual in astronomy, we use the terms ‘heavy elements’ and ‘metals’ to include all nuclei more massive than helium, although we will sometimes subject the noble gases (which do not interact chemically with the other elements to form solid condensates in the solar nebula and must be trapped instead) to special consideration.

Constructing planets via core accretion is a slow process, beginning only when the protostellar disk has cooled sufficiently for condensates to form (Lissauer, 1993; Safronov & Zvjagina, 1969). The main weakness of this model is that it may be difficult for planet formation to finish before disk dissipation occurs. As explored by Alibert et al. (2005), however, the formation time-scale may be shortened by invoking planet migration. Such movement through the disk brings a new supply of particles into the feeding zone of the growing planets, and therefore decreases the time required for them to be formed. Unfortunately, such complex variants of the planetesimal accretion model introduce more free parameters to the problem which are difficult to constrain for the early solar system.

1.2.2 Gravitational Instability

An alternative to the core accretion model has been proposed in the gravitational instability model. As the work discussed in this thesis adopts the core accretion formation mechanism, this alternative is only discussed briefly for completeness.

Studies have shown that this method, which does not require an initial core build-up phase, is capable of producing planets much faster than the core accretion scenario. The gravitational instability model instead posits that the thermal pressure is insufficient to support localized regions of the protoplanetary disk against gravitational forces. The regional instabilities collapse and condense to form giant gaseous protoplanets (the so-called ‘GGPPs’) on the order of a few times $\sim 10^3$ years (Boss, 1997).

This fast planet-forming mechanism is thus able to avoid the timescale

problem inherent in the previously discussed scenario; however, it is difficult to attribute the formation of the terrestrial planets to the same mechanism. For the purposes of this work, however, the important feature of the gravitational instability method is that giant planets are formed directly from the protoplanetary disk. As this disk contains the same chemical configuration as the nebula which condensed to form the Sun, it predicts that the planets possess near-solar metallicities.

1.3 Giant Planet Composition

1.3.1 Heavy Element Abundances from Observations

Elemental abundances in the upper atmospheres of the giant planets provide useful information pertaining to questions of planet composition, formation, and evolution. The data comes from a variety of instruments, including ground based telescopes, the Voyager Spacecraft, the Infrared Space Observatory, and the Galileo Probe. The elemental abundances are then determined through spectroscopic measurements of the observations (see Atreya et al. (1999) for a summary of the instruments and measurement techniques). With the exception of the Galileo Probe Mass Spectrometer (henceforth GPMS), which has had more widespread success, such analyses have primarily been useful in constraining the amount of carbon and nitrogen in the outer envelopes of Jupiter and Saturn. The observation which motivates this thesis is that the outer layers of both Jupiter and Saturn have been found to be significantly enriched in many elements by a factor of $\sim 3-7$ relative to solar abundances. The ratios to solar values are shown in Figure 1.1, while the manner in which the solar abundances are determined is outlined in Section 1.3.3, below.

The GPMS merits further mention, as it is responsible for the only *in situ* measurements of a gas giant planet. This probe, which entered the jovian atmosphere in 1995 (see Niemann et al. (1992) for overview of the mission and instrument), took measurements with unprecedented accuracy. The probe was also able to obtain measurements of elements which could not be measured using the spectral data: most notably, the noble gases were also shown to be present in super-solar quantities. The enrichment in noble gases provides an additional constraint on the manner in which heavy element accretion occurs, as noble gases are only trapped at low temperatures; it has been suggested that they therefore must have been accreted into the planetesimals at temperatures lower than 30K (Owen et al., 1999). The measurements from the GPMS are also shown on Figure 1.1. It should be noted

that the sub-solar neon abundance is frequently attributed to neon transportation to the unsampled inner region of the planet by helium droplets (Hubbard et al., 1999).

The oxygen value measured by the GPMS is also sub-solar, but this represents a strong lower limit on the actual oxygen abundance. The Near-Infrared Mapping Spectrometer on the Galileo orbiter demonstrated that the distribution of water in the jovian atmosphere is highly variable, and the probe is known to have sampled a particularly dry region. Since H₂O is the dominant oxygen carrier in the upper atmosphere, the water-poor entrance site resulted in a significant underabundance in the measured quantity of oxygen.

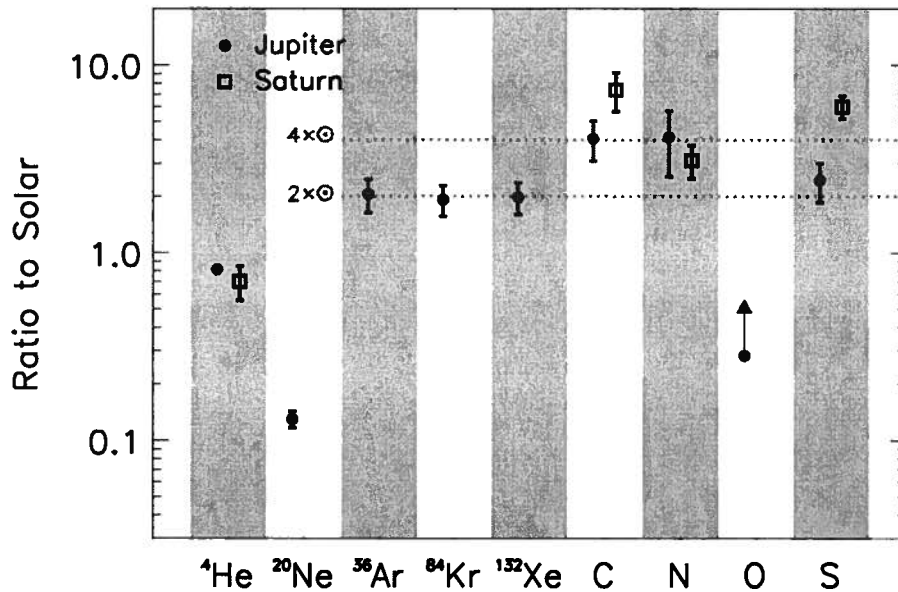


Figure 1.1: Elemental abundance ratios (relative to solar composition) for Jupiter and Saturn. See text and (Guillot, 2005)) for discussion of the data sources and measurement techniques. This plot (unpublished) provided by Tristan Guillot.

1.3.2 Envelope Enrichment from Structure Studies

While observations measure the quantity of metals in the upper planetary atmospheres, they are unable to independently constrain the global heavy

element abundances since they do not sample the inner regions of the planets. Even the Galileo probe only provided data to a depth corresponding to pressures of ~ 22 bar (~ 140 km). In order to obtain global quantities, it is therefore necessary to use atmospheric measurements in conjunction with interior models.

Giant planet interiors are thought to be made up of a cool outer layer composed primarily of molecular hydrogen, an inner region where hydrogen is in the form of ionized plasma, and a dense central core (Guillot, 1999b). Given that convection generally largely prevails in the envelopes of giant planets, especially at these young ages, one can certainly safely assume that the heavy-element ‘pollution’ was spread throughout the envelope. However there is no observational data for the innermost two regions, which make up the majority of the depth of the planet.

Since it is impossible to directly measure the chemical abundances in the inner regions of the planets, interior modeling relies instead upon other physical parameters including the planetary mass, equatorial radius, observed heat release from the planet, and gravitational moments (Guillot, 1999a). Models attempt to match these constraints to the theoretical predictions for a ‘self-gravitating and rotating fluid body in hydrostatic equilibrium’ (Chabrier & Küker, 2006).

One of the difficulties in modeling giant planet interiors arises from the range of conditions one encounters between the outer regions (pressure ~ 1 bar) and the core, where pressures are believed to exceed 10 Mbar (Chabrier et al. 2006). The phase transitions of hydrogen marks the boundary between the two outer layers, while the theoretical dense inner core is predominantly composed of heavy metals. As H is the dominant species, the most important piece of information is the equation of state of H at pressure of 1 - 10 Mbar. The equation of state then allows the connection between the observed surface data and the interior properties.

The interior models are subject to numerous uncertainties; it is difficult to determine how chemical species will behave in the densest regions of the planet. Recent laboratory experiments have made progress in investigating the behaviour of hydrogen in the limit of pressure-induced ionization but difficulties persist. The most notable example of the problems in this field are the inconsistencies between the equations of state of hydrogen derived using different laboratory methods (Chabrier & Küker, 2006). The problem becomes even more complicated when the other chemical species within the planet are considered. These uncertainties produce a range of acceptable values for the heavy element abundance in the planetary cores and envelopes. This is particularly problematic for Jupiter, as it is most affected by the

inconsistencies at high pressure.

1.3.3 Solar Composition

Information on the conditions in the protoplanetary disk is particularly useful to studies of the gas giant planets, as formation theories must be capable of constructing the planets from this environment in such a manner that they arrive at their current composition in the correct time interval. Although it is impossible to sample the protoplanetary nebula directly, CI carbonaceous chondrites² and current solar data are used to estimate the chemical and isotopic composition of the nebula from which the planets were produced.

By obtaining high-resolution spectra of the Sun, the abundances of certain chemical species can be determined. As the spectra are only representative of the solar photosphere, however, this method cannot measure elements that are not present in this region such as As, Se, Cr, Te, I, Cs, and the noble gases. Furthermore, the Sun has undergone significant evolution since the time of planet formation, with the spectra only supplying information on its current state. Solar evolution models must be used to convert measured values to those of the protosolar nebula. The necessity of such a conversion introduces a large amount of uncertainty into the method (see Lodders (2003) for discussion of this topic). Determining solar composition remains an area of ongoing research, with major adjustments recently being made to accepted values (Allende Prieto et al., 2002; Lodders, 2003).

CI carbonaceous chondrites are not believed to have undergone substantial transformation, and are therefore commonly adopted as fossil relics of the protoplanetary nebula. For many elements, CI chondrite measurements closely match those obtained from solar spectra, leading further credence to their status as early solar system relics. Although this method overcomes the need for modeling encountered with the stellar photospheres, it cannot be used for elements known to be depleted in meteorites, such as H, C, N, O, He, Ne, and Ar (Lodders, 2003).

1.4 Dynamical Models of Solar System Clearing

As outlined in Sections 1.2.1 and 1.2.2, the supersolar abundances of heavy elements found in the envelopes of the gas giant planets is not predicted by

² Like all carbonaceous chondrites, these objects are composed of a significant quantity of organic materials. CI chondrites have particularly high levels of water and are not thought to have undergone significant chemical alteration since the time of their formation

the dominant planet formation theories. This suggests that the surplus of metals was incorporated into the planets after most of the formation had occurred.

The forming, or newly-formed giant planets existed in a solar system populated by more planetesimals than remain today. As the solar system evolved, the majority of these small bodies were consumed by the Sun, accreted by a planet, or ejected from the system. During an impact with a gas giant, the planetesimal material is incorporated into the outer layers of the planet and spread throughout the envelope (as discussed in Section 1.3.2). A large quantity of such planetesimal impacts could then measurably increase the planetary metallicity, although it should be noted that many Earth-masses of arriving material are required for this to be the case.

The feasibility of this method of heavy-element transportation can be tested through dynamical simulations. The earliest stages of the formation of the solar system remain a matter of debate, however, and there are a variety of parameters that may be explored. The location and evolution history of the planets will alter the results, as will the state of the planetesimal disk at the commencement of the stage where the inter-planet planetesimals begin to be swept up. As a simple baseline, Guillot & Gladman (2000) investigated a scenario in which the giant planets begin with their current locations, masses, and radii. The 10000 test particles were massless and followed a r^{-1} heliocentric surface density profile from 4 to 35 AU. The 100 Myr simulation demonstrates that in this configuration, the planets are far too inefficient at accreting planetesimals to account for the surplus of heavy elements.

Following the stages of planet formation predicted by Pollack et al. (1996), Guillot & Gladman (2000) also analyzed the accretion efficiency of the giant planets during a period of formation in which they possess extended spherical envelopes measuring three times Jupiter's current radius. Jupiter and Saturn were assigned masses of $20 M_{\oplus}$, while Uranus and Neptune were assigned $10 M_{\oplus}$. The 10-Myr, 1000 particle simulation produced results consistent with the requirements for heavy element enrichment, but the envelopes lasted for a timescale greatly exceeding the expected contraction lifetime of the spherical envelopes. The problem thus becomes one of understanding how the planets efficiently accreted the planetesimal population.

Alibert et al. (2005) proposed a scenario in which the gas giant planets efficiently access the planetesimal population by migrating through the circumstellar disk. This method brings the planets to the planetesimals, unlike the previous scenario in which the growing planets gradually increase the planetesimal orbital eccentricities until their orbits intersect those of

the planets. The migrating planets (formed in a core-accretion scenario) in the Alibert et al. (2005) model travel several AU and efficiently accrete the planetesimals they encounter because the eccentricities, and thus relative speeds, remain small.

As discussed in Section 1.2.2, the gravitational instability scenario (Boss, 1997) posits very rapid giant-planet formation of a localized portion of the protostellar disk. Such a clump would share the same heavy-element abundances as the disk and therefore similarly poses the problem of transporting heavy elements to the planetesimals post-formation. Helled et al. (2006) studied the accretion efficiency of a gas giant planet forming by rapid ($\sim 3 \times 10^5$ yr) gravitational collapse. During this process, the protoplanet has an enlarged radius that increases its capture cross-section just as was the case with the extended envelopes described by Guillot & Gladman (2000). Under the assumption that planetesimals within the feeding zone of the collapsing protoplanet are not scattered outside of this region, Helled et al. (2006) found combinations of parameters producing accumulated planetary metallicities consistent with observations.

This thesis explores the possibility of using protosatellite disks as an alternate method for increasing the accretion efficiency of the giant planets. In this scenario (described in greater detail in Section 2, fewer free parameters are required than the more complex models discussed in this section.

Chapter 2

Methods

2.0.1 Solar System Model

Just as Guillot & Gladman (2000) determined that the heavy-element enrichment could not be caused by planetesimal pollution if the planets rapidly reached their current masses and radii at their current positions, we sought to investigate if the presence of a protosatellite disk could enhance the planet's cross-section to enable sufficient planetesimal capture. Although there are many parameters in the problem, this thesis looks at what the literature offers as reasonable values for surface densities, planetesimal sizes, etc., and calculates the enrichment. Our base scenario is along the lines of the 'simplest thing one could imagine', and we find that the results are in agreement with the known constraints.

Broadly, we studied the scenario in which the protoplanetary cores of the four giants grow close to their current locations (migration of Uranus and Neptune is not incorporated, but see Section 4). We have numerically verified that during the phase in which the planets are still cores, the orbital instability time scale between the planets is longer than the $\sim 1 - 3$ Myr expected time scale for dissipation of the protosolar disk (Haisch et al., 2001), and thus little inter-planet clearing occurs (see A.1). The two gas giants then rapidly acquire their gas disks (Pollack et al., 1996) at which point their gravitational perturbations rapidly ($10^5 - 10^6$ yr) clear the regions between them (Franklin et al. (1989), Gladman & Duncan (1990)). However, during this stage where the gas giants have accreted most of their mass but gas is still present, the planets will be surrounded by dense protosatellite disks. The planetesimals between the planets have numerous close planetary encounters before they can be cleared, and they will see high gas densities (which may alter their motion) as they fly through the protosatellite disks. These disks are believed to persist for $\sim 1 - 10$ Myr (which is obviously the same as the time scale over which the Sun's disk remains).

We have therefore studied the effect of protosatellite disks on the dynamics of the planetesimals to see if the passage through these disks can increase the flux of material incorporated into the planetary envelopes. This scenario

fits nicely into the hypothesis that multiple generations of satellites formed and then migrated into the planetary envelopes (*e.g.* Canup & Ward (2006)), with the disks serving as nets through which large amounts of material are cycled into the planets. The simulations which are the focus of this paper distributed non-interacting test particles between 4 and 35 AU on circular orbits. The justification for setting the initial planetesimal eccentricities (e_0) to be negligible is explored below in Appendix A.2. The particles served as tracers of the heavy elements in the disk, with the surface density of these heavy elements being distributed according to the power law:

$$\sigma = \sigma_5 \left(\frac{r_{\text{AU}}}{5 \text{ AU}} \right)^{-1} \quad (2.1)$$

The surface density has been normalized to $\sigma_5 = 10 \text{ gcm}^{-2}$, a commonly-used value for $r \sim 5 \text{ AU}$ (Pollack et al., 1996). From this initial distribution, the quantity of heavy elements required to form the cores of each of the giant planets was removed assuming planetesimal incorporation into the core was essentially 100% efficient. This material was extracted symmetrically around the current semimajor axis using the width Δa needed to build the core. The mass of the saturnian core suggested by models is $15 M_\oplus$, while the core mass of Jupiter is more dependent on the adopted equation of state (EOS), with estimates varying between 0 and $15 M_\oplus$. We therefore investigate a number of possible jovian core masses in this range: 0, 2, 5, 10, and $15 M_\oplus$. A mass of $10 M_\oplus$ was removed for each of the ice giant planets. Fig. 2.1 illustrates the surface-density profiles of the disk after the heavy elements have been removed for the cores. A total of $150 M_\oplus$ heavy elements remains in the disk after the removal of mass for the cores of Saturn and the ice giants.

After extracting the cores, the interplanetary region is populated with the non-interacting³ tracer particles. For each planet, the fraction of impacting tracers (as a function of initial heliocentric distance) is logged which in turn allows us to calculate the total amount of accreted heavy elements. We investigate three general scenarios for planet formation, with the goal of keeping the models reliant on a small number of free parameters. The base-line case populates the current Solar System with the circumsolar disk of planetesimals, effectively recreating the study undertaken by Guillot & Gladman (2000) as a check. In our main study, the planets possess short-lived protosatellite disks. Finally, we investigate the affect of a delay between the onset of runaway gas-accretion for Saturn (after that of Jupiter).

³These massless point particles interact only with the giant planets and the sun, not with each other

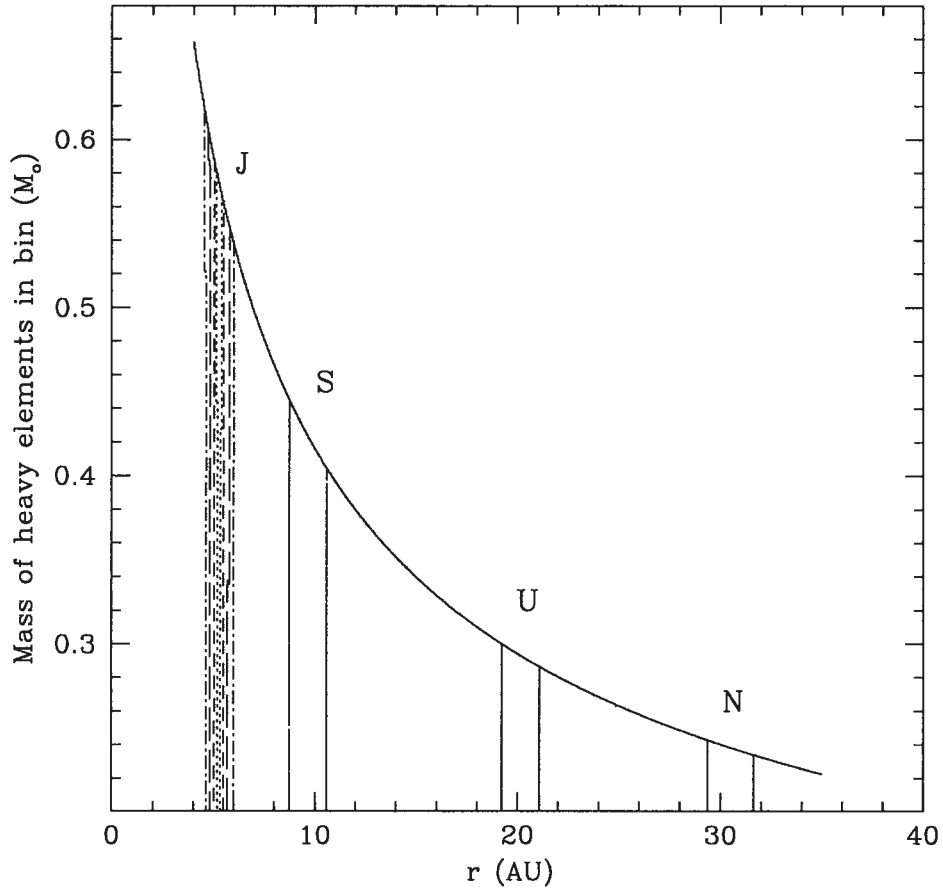


Figure 2.1: Depiction of the heavy-element distribution in the protoplanetary disk. Solid line corresponds to the original heavy element surface density. The amount of heavy elements removed for the jovian core was as follows: $2 M_{\oplus}$ (dots), $5 M_{\oplus}$ (short dashes), $10 M_{\oplus}$ (long dash) and $15 M_{\oplus}$ (dot-dash). $15 M_{\oplus}$, $10 M_{\oplus}$, and $10 M_{\oplus}$ were removed for the cores of Saturn, Uranus and Neptune respectively.

2.0.2 SWIFT RMVS3 Symplectic Integrator

Like all N-body dynamical problems, investigating the orbital evolution of planetesimals in the outer solar system cannot be done analytically. Although there are several approaches to undertaking these simulations, the use of symplectic integrators is frequently adopted in solar system dynamics research. This is the method employed herein and is discussed briefly below.

We use the SWIFT RMVS3 symplectic integrator to conduct our numerical simulations. This program was specifically developed by Harold Levison and Martin Duncan to handle ‘small objects on timescales approaching the age of the solar system, while also being able to follow the important, but short-lived close approaches between these objects and planets’ (Levison & Duncan, 1993). This is done by using more than one time step size - a small time step is used during a close encounter to ensure accuracy, while a larger time step allows the simulation to progress quickly when no such interaction is taking place. An RMVS (Regularized Mixed Variable Symplectic) integrator switches from a heliocentric to a planetocentric frame of reference for a particle located within 1 Hill radius from a planet. See Levison & Duncan (1993) for more details on RMVS symplectic integrators in general and SWIFT in particular.

The number of particles in each simulation exceeded 110,000 although the exact number was dependent on the computational resources available at the commencement of the simulation. All simulations proceeded for 150 Myr with a base time step of 0.25 yr. Particles were stopped when they struck a planet, dropped below 0.4 AU or traveled beyond 1000 AU. The planet that accreted the particle and the time of the accretion are logged in a separate file.

Most critically for our study, we also log information for each ‘close encounter’ that a particle experiences with a planet, defining this term to mean any trajectory that causes a test particle to come within 0.1 AU of a planet. At each such passage, we record the planet with which the encounter was had, the time of the encounter, the pericentric distance, and the particle’s planetocentric position and velocity vectors at an instant close to pericenter (see Appendix A.3 for justification of this approach). With these quantities, we are able to reconstruct the nature of the planetocentric orbit causing the close encounter. As expected, the majority ($\sim 60\%$) of the particles were on hyperbolic orbits with respect to the planets, with the orbital inclination with respect to the disk distributed isotropically (see Appendix A.4).

2.0.3 Experimental Hardware

All simulations were run on the 170-CPU Beowulf cluster ‘LeVerrier’ housed in the Planetary Science laboratory at the University of British Columbia. This cluster is composed of 94 Athlon 2600-MP CPUs and 76 Opteron 2.2 GHz 64-bit CPUs; both types of CPUs were used throughout the course of this research. Each of our 150 Myr simulations represent approximately 8 years of CPU time. Having conducted 5 simulations of this length, as well as several shorter tests, the simulations on which this thesis is based are the product of over 40 years of CPU time.

Chapter 3

Results

3.1 Baseline case

Guillot & Gladman (2000) investigated the planetesimal accretion efficiency of the gas giants under the approximation that the time until they reach their current mass and radius is negligible compared to the time needed to destabilize the planetesimal disk. They integrated 10,000 planetesimals for 100 Myr and demonstrated that the accretion efficiency in such a scenario is too low to be consistent with estimated planetary metallicities. Only 4% of the particles struck one of the giant planets, while 84% were ejected to the Oort cloud or beyond.

We reproduce this simulation, integrating 167,400 test particles for 150 Myr. Confirming the results of Guillot & Gladman (2000), we find that the gas giants accrete an insufficient amount of heavy elements. For any of the four Jupiter core masses used in this study, only 3 – 5% of the particles impact one of the giant planets. The metallicity of Jupiter and Saturn are only marginally increased by these few planetesimals, adding only $2.9 M_{\oplus}$ and $0.7 M_{\oplus}$ worth of heavy elements respectively. This enhancement is significantly lower than the minimum enrichments of $\sim 5 M_{\oplus}$ and $\sim 1 M_{\oplus}$ needed by models of interior structure.

Although the simulation ran for 150 Myr, the giant planets accumulate most of the planetesimals in the neighbourhood of their cores within the first 0.15 Myr of the simulation (see solid black and shaded histograms in Fig. 3.1); the later stages of the simulation are dominated by the gradual arrival of the planetesimals that originate in the neighbourhood of the two ice giant planets. As the system evolves and the majority of the planetesimals are accreted by the planets or are removed from the planetary region of the solar system, the rate of arrival of planetesimals to the gas giants decreases. At 150 Myr, the planetary region of the Solar System has been largely cleared of planetesimals.

As discussed in Guillot & Gladman (2000), Jupiter is particularly efficient at ejecting particles from the system, making it difficult for the giant planets to accrete material while the availability of the planetesimals makes

it favourable to do so. For the heavy-element surplus of the gas giants to be attributable to pollution by the planetesimals in our protoplanetary disk, the accretion efficiency must be enhanced - particularly during the early stages of dynamical evolution. Guillot & Gladman (2000) suggested that enlarging the planetary radii would increase the capture cross-section of the planets. We propose that the presence of short-lived protosatellite disks as a simple alternative method for increasing the giant-planet accretion efficiencies.

3.2 Protosatellite Disks

3.2.1 A simple protosatellite disk model

The presence of a massive protosatellite disk would increase the effective capture cross-section of the planet during the crucial period of planetesimal sweep-up. Recent estimates place the mass of solids in such protosatellite disks on the order of a few times 10^{-4} the mass of the host planet (M_{pl}) with a gas-to-solids mass ratio on the order of 10^2 (Canup & Ward, 2006). We adopt disk masses of $0.02 M_{pl}$, extending out to 30 planetary radii (r_{pl}), and height to radius ratio of 0.1 (corresponding to an opening angle of $\sim 6^\circ$). The disks are placed parallel to the planet's orbital plane with a surface density dictated by an r^{-1} power law.

The radius of each planetesimal is randomly selected from a power-law size distribution $N(D) \propto D^{-q}$, with radii between D_{min} and D_{max} . In the absence of direct constraints on the size distribution of planetesimals in the early Solar System, the slope value is taken to be $q=4.25$ from the most current estimate for the size distribution of the Kuiper Belt (Fraser et al., 2008). If collisional evolution has modified the current distribution, the most likely result would be a steeper primordial distribution. At these slopes, the majority of the system mass is in the smallest planetesimals. The value on D_{max} then becomes essentially irrelevant and so we take $D_{max}=4000 \text{ km} \approx 2 \times R_{Pluto}$, since it has a negligible probability of selection. As shown in Fig. 3.2, the results of our study are not highly sensitive to the selection of D_{min} as long as this value remains in the $\sim 30 \text{ km}$ range. We therefore adopted $D_{min} = 30 \text{ km}$ for the work presented in this thesis. The density of the planetesimals is taken to be 1 g cm^{-3} .

The trajectories of the test particles through the protosatellite disk are naturally divided into two regimes: those in which the planetocentric orbital inclination with respect to the disk exceed the opening angle of 6 degrees, and those that travel along the plane of the disk. When $i > 6^\circ$, the path length through the disk is approximated as twice the scale height; the total

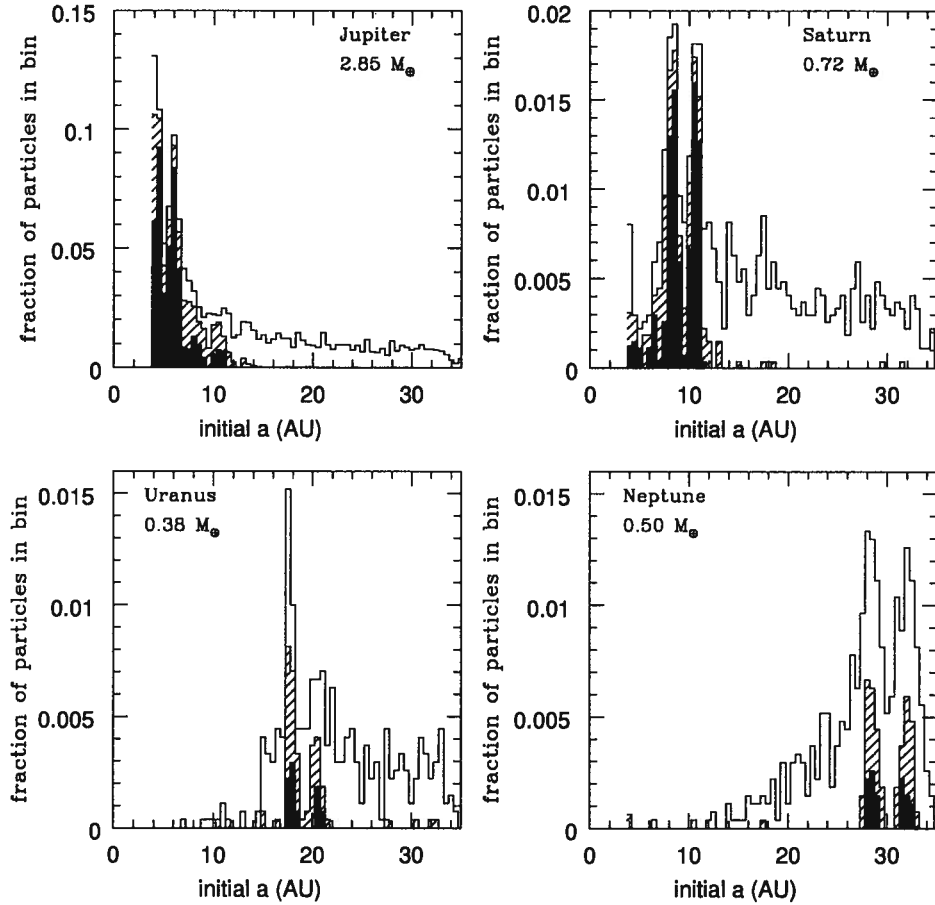


Figure 3.1: Heavy-element accumulation efficiencies as a function of initial planetesimal semi-major axis (a_o) for the 4 giant planets. All of the giant planets possess their current radii and masses for the duration of the 150 Myr simulation. The stacked histograms correspond to particles accumulated before 0.015 Myr (solid), between 0.015 and 0.15 Myr (dashed), and between 0.15 and 150 Myr (white). See text for explanation of the initial heavy-element distribution for the 167400 test particles. The giants accumulate most of the planetesimals in the neighbourhood of their cores within the first 0.15 Myr of the simulation.

amount of mass encountered by such a particle as it traverses the disk is calculated using the surface density of the disk at the nodal point of the close encounter (see Equation 2.1). The calculation of the path-length during a low-inclination encounter is more complex. We approximate the length of the in-disk trajectory as equal to the linear path through the disk with the same pericenter distance. Due to the fact that the transit speeds through the disk are measured in km/sec (and thus much faster than the sound speed of the disk's gas) we use the common approximation that the planetesimal absorbs the encountered gas mass and slows down via simple linear momentum conservation.

Knowing the orbital parameters before disk passage and the absorbed mass, we calculate the transfer of momentum and thus the post-encounter planetocentric velocity. The nature of the post-passage planetocentric orbit is then determined and the total heavy-element content of any planetesimal that strikes the planet directly or is captured onto a bound planetocentric orbit through interaction with the planetary disk is considered to be accumulated by the planet. Any bound orbit will eventually make multiple disk passages and be drawn into the disk. It is therefore more difficult for the planetesimals to accrete larger (and thus more massive) planetesimals through this mechanisms than the smaller particles (see Fig. 3.2).

If a particle passes through the disk and remains unbound from the planet, we do not alter its orbit to reflect the exchange of momentum that took place during the passage. Our calculated accreted metallicities are therefore conservative, as they are lower than would be the case had this calculation been done. As shown in Figure 3.2, however, the number of particles passing through the jovian disk without subsequently being accreted by Jupiter (right-most panel) are dwarfed by the number of particles that are accreted (first two panels). This suggests that our results are not significantly affected by our neglect of the mass-transfer to particles passing successfully through the disk.

3.2.2 Simultaneous formation of Jupiter and Saturn

We increase the complexity of our Solar System model by adding protosatellite disks (as described in Section 3.2.1) around Jupiter and Saturn. The duration of such protosatellite disks is constrained by formation-time estimates of the regular satellites. Callisto, for instance, is believed to be at least partially differentiated (Anderson et al., 2001); this places a natural lower-limit on the accretion time-scale of the satellite, as very rapid formation would cause it to melt, thereby causing it to become undifferen-

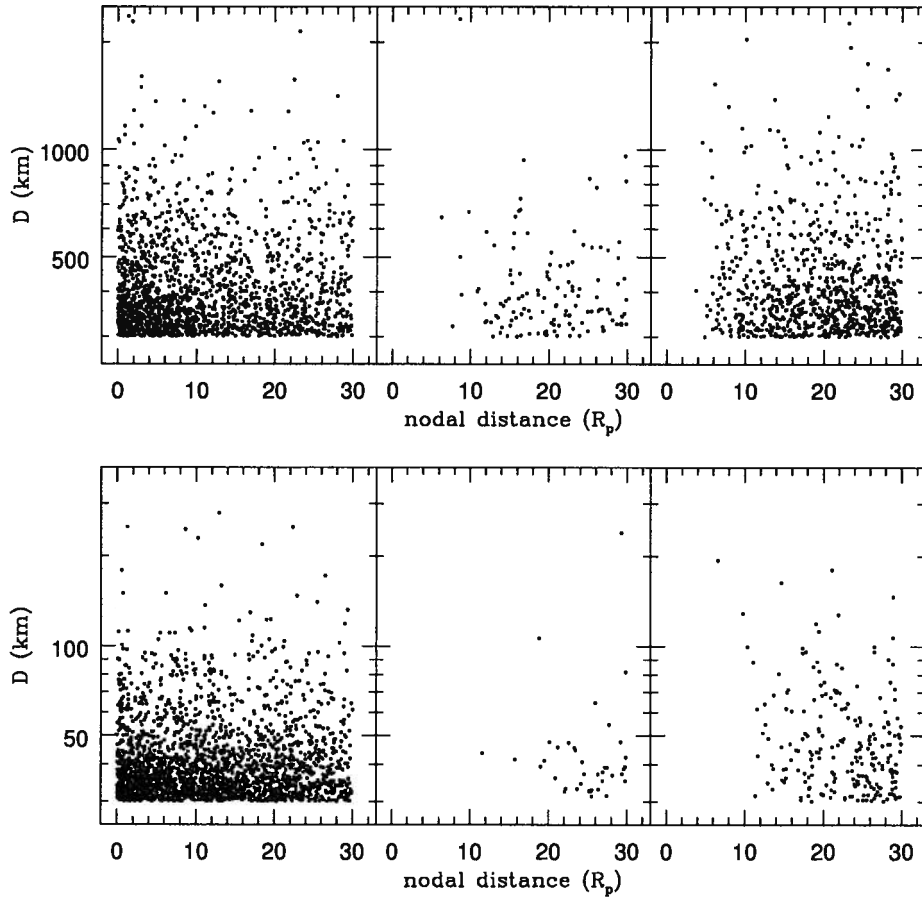


Figure 3.2: Distribution and fate of planetesimals passing through the jovian protosatellite disk. The upper row corresponds to a minimum planetesimal diameter of 300 km, while the lower row has $D_{min} = 30$ km. Horizontal panels (left to right) represent particles placed on bound orbits that are thus accreted by the planet, passage of particles that make it through the disk but are later accreted by Jupiter, and particles that pass through the disk and are never accreted by Jupiter. When the minimum diameter of the test particles descends to 30 km, over 90% of the disk passages result in accretion. This indicates that the results of the calculations are not sensitively dependent on the minimum diameter, assuming that this value is in the ~ 30 km range (the value we adopt in this study).

tiated. By extension, the duration of the protosatellite disk must similarly adhere to this lower-limit. The satellite formation models of Mosqueira & Estrada (2003) form Callisto in ~ 1 Myr; similarly, the results of Barr & Canup (2008) place a minimum accretion timescale on Callisto of ~ 3 Myr. Although most likely values for the protosatellite disk lifetimes range from 1 to 10 Myr, we investigate the sensitivity of the final metallicity on this parameter by varying the disk lifetime from 0.1 Myr to 100 Myr, taking 3 Myr as our nominal value.

The protosatellite disks significantly enhance the accretion cross-sections of the giant planets, with longer-lasting disks predictably resulting in higher planetary metallicities. Even the relatively short-lived 0.1 Myr disks produce envelope metallicities of $11.5 M_{\oplus}$ and $3.9 M_{\oplus}$ for Jupiter ($5 M_{\oplus}$ core) and Saturn respectively. Adopting a more massive jovian cores cause the envelope of Jupiter to be moderately less enhanced in heavy elements, as expected. A more likely disk lifetime of 3 Myr increase these values to 18.6 and $6.4 M_{\oplus}$ (see Fig. 3.3). This marks a significant enhancement over the parallel baseline scenario, in which Jupiter and Saturn accumulate $2.9 M_{\oplus}$ and $0.7 M_{\oplus}$. As with the base-line case, however, particles are quickly removed from the inner regions of the Solar System. This causes the rate of increase of metallicity as a function of protosatellite disk duration to decrease with time (see Fig. 3.4).

Theoretical estimates of the heavy-element content in Jupiter’s envelope range from $\sim 6 - 37 M_{\oplus}$ and as such provide only weak support for the validity of our model. The interior models of Saturn are much better constrained, producing estimates of $\sim 1 - 8 M_{\oplus}$, and therefore are a more useful tool in identifying the more favourable models. For instance, disks lasting longer than $\sim 1 - 3$ Myr begin to move Saturn’s accumulated metallicity towards the upper limits of the predictions (see Fig. 3.4). This could be problematic, as work based on the differentiated state of Callisto and Rhea suggest that gas disks remained in place around Jupiter and Saturn for at least 3 Myr (Barr & Canup, 2008), but there is no great cause for concern given current uncertainties.

At this stage, we also investigated the dependence of our results on disk mass. The metal enrichment of Jupiter is relatively weakly dependent on the chosen mass of the protosatellite disk: while increasing the mass by a factor of 10 only increases the metallicity by $\sim 6\%$; the saturnian metallicity was more significantly affected by a similar increase in the disk mass, having a heavy-element increase of 25%. Alternatively, decreasing the disk masses by a factor of ten drops the jovian and saturnian metallicities by 19% and 27% respectively.

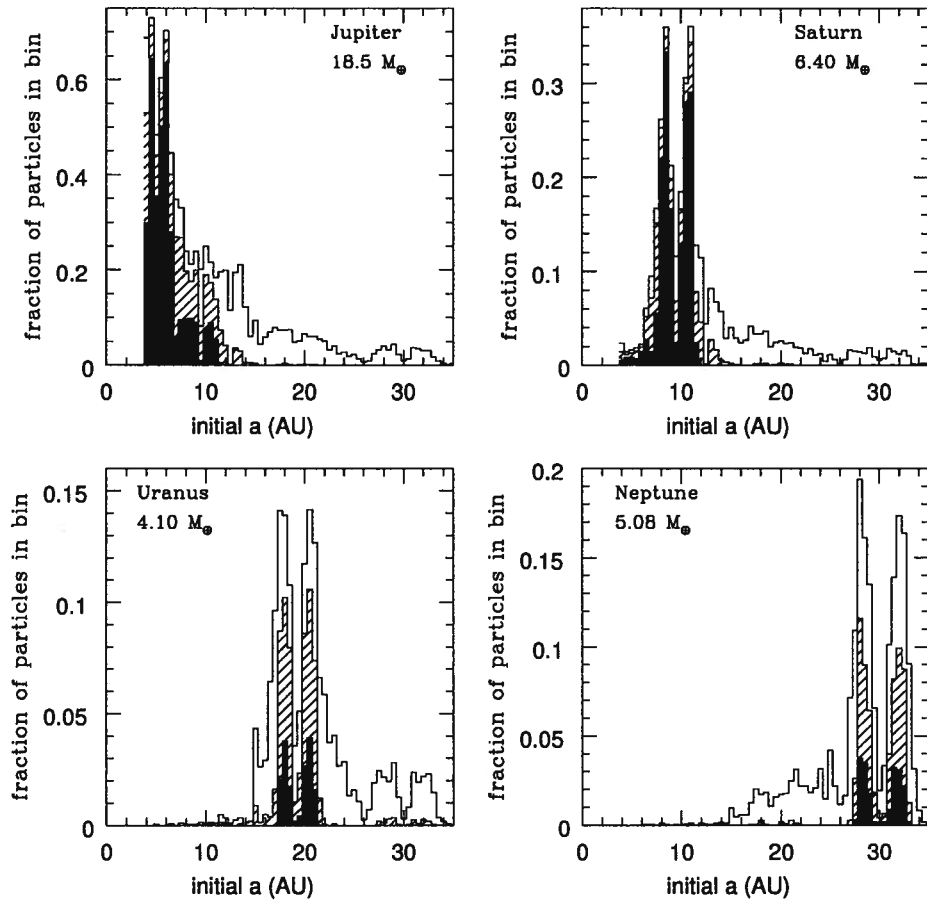


Figure 3.3: Heavy-element accumulation efficiencies as a function of a_0 for the 4 giant planets. The onset of runaway gas accretion for Jupiter and Saturn is taken to be simultaneous and both possess protosatellite disks for the first 3 Myr of the simulation. See Fig. 3.3 for explanation of histogram shading.

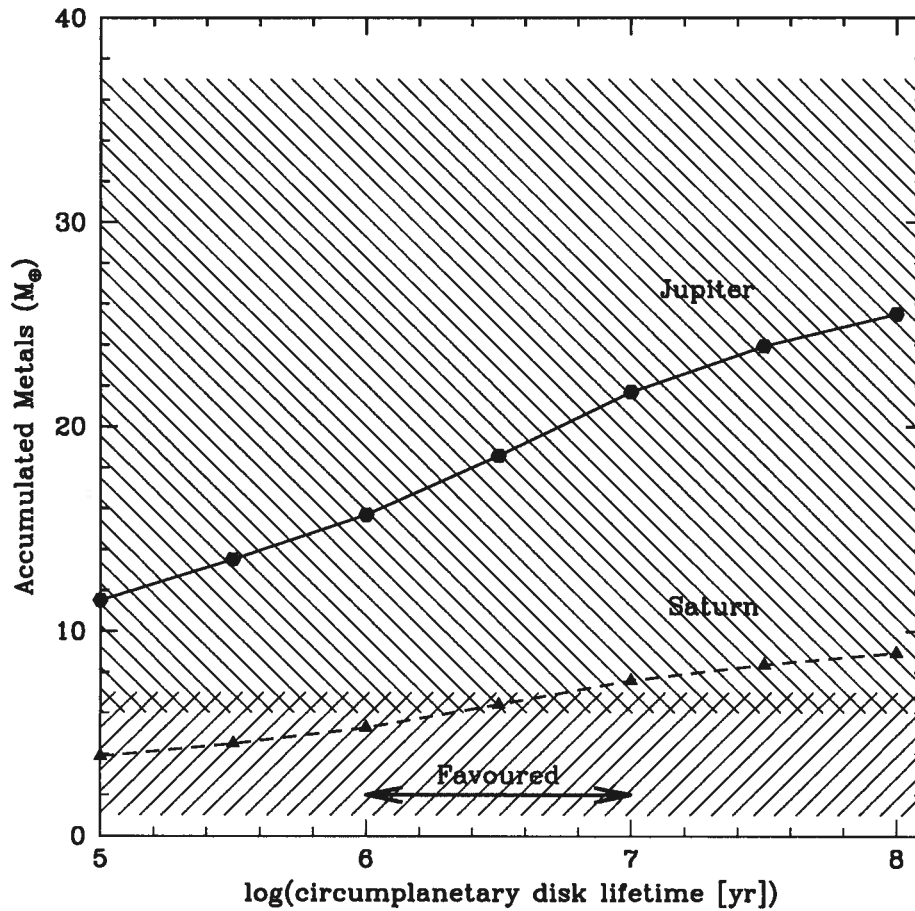


Figure 3.4: Planetary heavy-element enrichment as a function of protosatellite disk lifetime. The amount of accreted heavy elements increases with disk lifetime, although the presence of the disk becomes less significant as time progresses and the planetary region of the solar system becomes substantially depleted in planetesimals. Recent studies (Barr & Canup, 2008; McKinnon, 2006; Mosqueira & Estrada, 2003) place a lower limit of ~ 3 Myr on the protosatellite disk duration. The allowed range of metallicities for Jupiter and Saturn are shaded (slanted left and right respectively). The metallicity of Saturn approaches the upper limit as the disk lifetime exceeds ~ 10 Myr.

3.2.3 Evolution of Uranus and Neptune

The composition and internal structure of Uranus and Neptune are more speculative than those for Jupiter and Saturn, since the values required to derive these properties - such as gravitational moments - are more uncertain for the ice giants than their gaseous counterparts. Despite the lack of reliable estimates of core mass and heavy element enrichment do not exist, a few general properties of the ice giants can be ascertained. For instance, assuming that the ice giants possess the protosolar ice/rock ratio, models dictate that both should be made up of 5 - 15% hydrogen and helium by mass (Guillot, 1999b). Using their current masses, this implies a total H + He mass of 0.7 - 2.2 M_{\oplus} and 0.9-2.6 M_{\oplus} for Uranus and Neptune respectively.

For the entirety of each of our simulations, both Uranus and Neptune possess their current masses (14.53 M_{\oplus} and 17.14 M_{\oplus} respectively). From the initial distribution of heavy-elements in the proto-planetary disk, we remove 10 M_{\oplus} for each of the ice giant cores. In the scenario in which all giant planets possess protosatellite disks for 3 Myr, Uranus accumulates 4.1 M_{\oplus} of heavy elements, while Neptune acquires 5.1 M_{\oplus} . These enrichments, when added to the cores and the light element masses, raise the calculated masses of the ice giants into the realm of their measured values. Furthermore, our model naturally results in a mass for Neptune exceeding that of Uranus, mirroring what is observed.

3.2.4 Delayed formation of Saturn

The case described above adopted the assumption that Jupiter and Saturn gained their gas envelopes and protoplanetary disks concurrently. Although the results are consistent with the constraints, the heavy-element enrichment of Saturn's envelope approaches the maximum limit dictated by the models. It is conceivable, however, that the two gas giant cores did not acquire their gas envelopes simultaneously, with Jupiter evolving faster than Saturn. During this epoch, a disk-endowed Jupiter is able to sweep up some of the planetesimals that Saturn (present only as a core) is unable to accrete. The core of Saturn efficiently scatters rather than accretes the nearby planetesimals. In many cases, the eccentricities induced by Saturn are sufficient to place the planetesimals on Jupiter-crossing orbits. Jupiter accretes some of these planetesimals, and those heavy elements are no longer available for Saturn to absorb once it acquires its protosatellite disk.

For clarity, the values used in the following discussion are once again those for a 5 M_{\oplus} jovian core mass and a protosatellite disk lifetime of 3

Myr. The plausible offsets between the full formation of Jupiter and Saturn are uncertain, warranting an investigation both of the resultant metallicities of the gas giants and the sensitivity of the results to the delay duration. To enable such a study, we adopted delay times covering almost two orders of magnitude: 0.03, 0.1, and 1 Myr.

Since Jupiter efficiently removes planetesimals from the neighbourhood of the gas giants soon after formation, the short 0.03 Myr delay in the formation of Saturn measurably alters the final composition of the planet, lowering its metallicity from $6.4 M_{\oplus}$ to $4.7 M_{\oplus}$. Even the 1 Myr delay, however, still allows Saturn to accumulate $4.55 M_{\oplus}$ of heavy elements. The results from the 0.1 Myr delay are shown in Fig. 3.5 and demonstrate that such an offset allows both gas giants to accumulate sufficient quantities of heavy elements while at the same time preventing Saturn from becoming too enriched. It is interesting to note that this is similar to the 0.2 Myr offset used in the Alibert et al. (2005) model, under a dramatically different physical scenario.

Essentially Saturn’s bare core (whose escape speed is large relative to the local orbital speed around the Sun) efficiently scatters rather than accretes nearby planetesimals; the induced eccentricities are sufficient in many cases to cross Jupiter’s orbit. Thus Jupiter obtains some of these heavy elements and they are no longer available for Saturn to absorb once it acquires its protosatellite disk.

3.2.5 Mass transfer to the outer Solar System

Planetesimals were removed from our simulations if their heliocentric distances exceeded 1000 AU; because the velocity was recorded at the time that this condition is met, we are able to determine if each such planetesimal was on a bound or unbound orbit at the time of removal. For our ‘standard’ simulation of 3-Myr disk duration (with no Saturn delay) and a five Earth-mass jovian core, the planetesimal population initially has $145 M_{\oplus}$ of material. At the end of the 150-Myr simulation (see Fig. 3.6), we find that $\simeq 2M_{\oplus}$ of material has been removed from the interior boundary (from a variety of initial semimajor axes), that only $\simeq 13M_{\oplus}$ remain ‘alive’ at the end of the simulation, and that $\simeq 6M_{\oplus}$ of this material is at distances between 40 and 1000 AU. The $\simeq 7M_{\oplus}$ of material interior to a distance of 40 AU is predominantly trapped in the Trojan points of Jupiter or Neptune, surviving at the inner edge of the Kuiper Belt outside $\simeq 34$ AU where it becomes stable (Levison & Duncan, 1993), or in the metastable region near 26 AU where it is stable for these time scales (Gladman & Duncan, 1990).

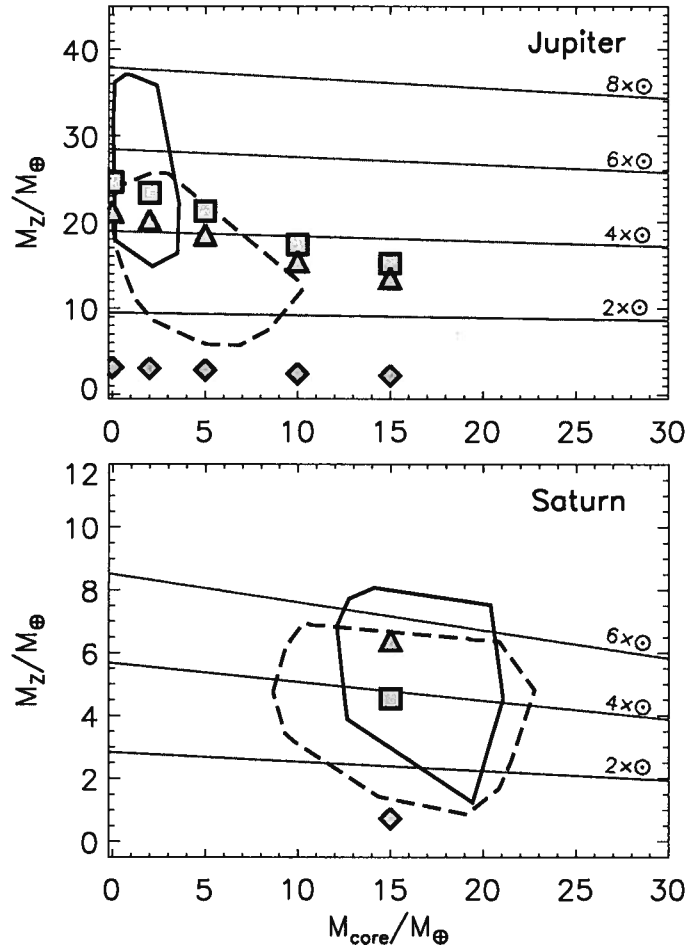


Figure 3.5: Comparison of the constraints on planetary metallicities from observation and modeling of the planets to those produced by our three cases: no-disk (diamonds), 3 Myr circumplanetary disk (squares), and 3 Myr circumplanetary disk combined with a 0.1 Myr delay in the onset of runaway gas-accretion in Saturn (triangles). The horizontal axis gives the heavy-element mass of the core, while the vertical axis is the heavy-element mass of the planet’s envelope. Dashed and solid borders correspond to constraints from interior models derived with different equations of state. The nearly-horizontal grey lines indicate heavy-element abundances within the envelope that are indicative of enrichment by specific factors relative to solar (factors as labeled). See Guillot (2005) for discussion of the models used to produce predicted metallicities.

The lower right panel of Fig. 3.6 shows the radial distribution of the surviving planetesimals at 150 Myr. Most of these objects come from initial locations exterior to 15 AU, building a scattered disk dominantly from the 15-33 AU region. The radial distribution of this material is roughly similar to that found by Duncan & Levison (1997) after scattering simulations that lasted 4 Gyr. Converting to surface density, our simulation has roughly a factor of 30 drop between 50 and 200 AU, as found by Duncan & Levison (1997). From 200 – 1000 AU our drop is a factor of 2 less steep than the earlier work, but we have not dynamically eroded our population for the following 4 Gyr, and these more weakly bound particles may be preferentially lost, making direct comparisons difficult. However, if we take the $\sim 1\%$ survival rate estimated by Duncan & Levison (1997) for these particles, the current mass expected to be in the scattering population from this simulation would be $\sim 0.05 M_{\oplus}$, in agreement with the Trujillo et al. (2000) estimate of $\sim 0.06 M_{\oplus}$ for this population.

What effect does our protosatellite disk hypothesis have upon the ejection of material from the Solar System? The upper right panel of Fig. 3.6 shows the initial locations for particles ejected hyperbolically (lower histogram) and for those particles sent past 1000 AU on bound orbits (upper histogram). $30 M_{\oplus}$ of planetesimals are ejected, while planetesimals with $57 M_{\oplus}$ reach 1000 AU on bound orbits. Our study can be compared to that of Hahn & Malhotra (1999), who studied delivery to the Oort cloud from a dispersing outer Solar System disk; our simulation with $145 M_{\oplus}$ of planetesimals outside the initial cores is about halfway between their 100 and $200 M_{\oplus}$ cases. Hahn and Malhotra stopped particles at 3000 AU, whereas we stopped them at 1000 AU; however, we will take the $r > 1000$ AU objects to be those which are deposited later in the Oort cloud. Like Hahn and Malhotra, we find that the initial region between Saturn and Neptune would dominantly supply the Oort cloud. We also find the similar result that as time progresses, the ratio of objects deposited on bound orbits outside 1000 AU to those ejected to be roughly constant in time. However, while Hahn & Malhotra (1999) find the ratio of mass beyond 3000 AU to the ejections to be ~ 0.4 , we find the ratio to be ~ 2 . This is largely because the presence of the protosatellite disks provide a ‘rate limiting’ process which lowers the fraction of ejections during the initial period when the planets initially clean out the disk. The very-close planetary flybys which are the most effective at boosting planetesimals to unbound orbits via gravity assists are those which are now preferentially absorbed by the disks. Thus, the scenario we posit greatly increases the efficiency of planet formation, since our $145 M_{\oplus}$ disk ‘wastes’ only $30 M_{\oplus}$, putting $\simeq 34 M_{\oplus}$ of the material into

the planetary envelopes. Without disks, the planets in Hahn & Malhotra (1999) simulations eject about 70% of the planetesimals, or about $105 M_{\oplus}$ from a $145 M_{\oplus}$ disk. In terms of absolute mass of the Oort cloud, only about 0.1–0.5 of the $57 M_{\oplus}$ of the $r > 1000$ AU particles need reach the Oort cloud to supply a cloud in the 5–30 M_{\oplus} range, as discussed by Hahn & Malhotra (1999).

3.2.6 Compact Configuration

Many models of the development of the solar system have difficulty accounting for the current non-negligible eccentricities and inclinations of the giant planets. A simple scenario in which the planets form close to their current locations seems to predict that one would expect to find them on circular, co-planar orbits. The so-called ‘Nice Model’ proposes an alternative history for the solar system, and is notable for its ability to produce planets on moderately eccentric, inclined orbits. Briefly, this model posits that giant planets initially form much closer to the Sun and each other. From this initial compact configuration, the planets naturally evolve outwards upon interaction with the surrounding disk, and it is this dramatic orbital evolution that is capable of reproducing the current configuration of the solar system (Tsiganis et al., 2005). The model is also of interest because it can be used to explain other events that occurred in the developing solar system (see for instance Gomes et al. (2005) and Morbidelli et al. (2005)).

When beginning from a compact configuration as required by the Nice model, less mass is present in the inter-planetary regions in the form of planetesimals. Since one might expect it to be more difficult for the planets to enhance their envelope metallicities to observed values through planetesimal accretion in such a scenario, we investigated the capture efficiency of the giant planets in the initial positions predicted by the Nice model assuming they each possess protosatellite disks as described in Section 3.2.1.

The planets were laid out at 5.45 AU (Jupiter), 8.18 AU (Saturn), 11.5 AU (first ice giant planet), and 14.2 AU (second ice giant). We distributed 520 massless test particles between 4 and 30 AU. After the integration ran for 100 Myr, the inter-planetary regions were largely void of planetesimals while the material from the exterior region ($a > 20$ AU) could not be accessed by the planets. We then calculated the mass of heavy elements accreted by each planet using the procedure described above. With 3 Myr disks, Jupiter and Saturn accreted $\sim 10 M_{\oplus}$ and $\sim 6 M_{\oplus}$ of heavy elements respectively, which (as shown in Fig. 3.5) are acceptable matches to the constraints. This investigation demonstrates that the simple disk model is capable of

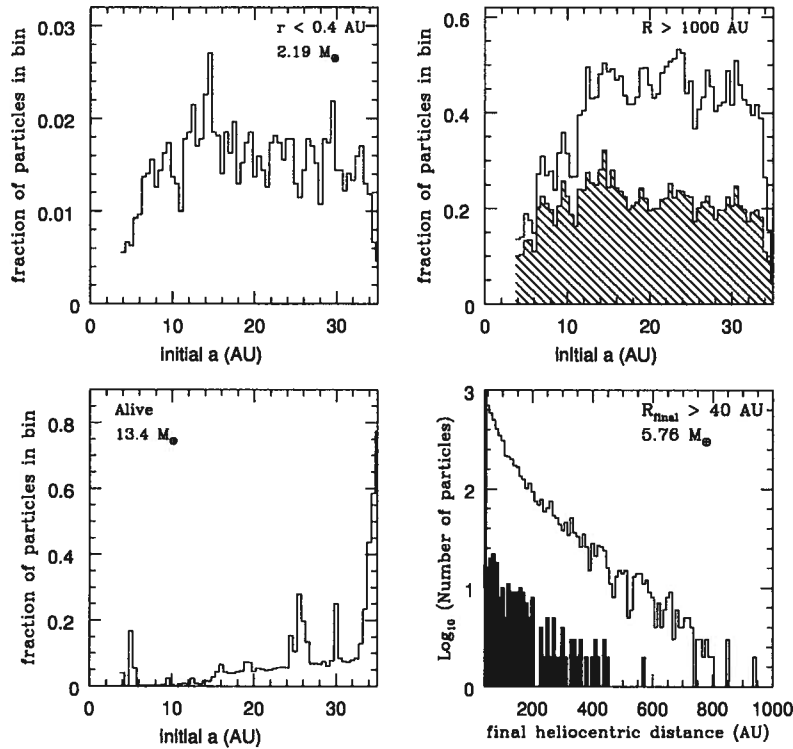


Figure 3.6: Final distribution of planetesimals that are not accreted by a planet for the scenario discussed in Fig. 3.3. Top left: initial a for particles striking the Sun. Bottom left: The *initial* semimajor axes for particles still in the simulation at 150 Myr. Bottom right: histogram of number of particles as a function of distance at 150 Myr in the 40 – 1000 AU range. The solid histogram shows the subset of those particles which began with $a < 15$ AU. Top right: Dashed histogram shows the initial a for particles ejected hyperbolically from the Solar System. The upper histogram (*not* a stacked histogram) gives initial a for particles removed for reaching 1000 AU but which were dynamically bound at that time. The ejected particles are seen to be only about half as numerous as the bound particles.

accounting for the heavy-element enrichment of the gas giants in either a compact or non-compact initial configuration.

Chapter 4

Conclusions

Our main conclusion is that protosatellite disks (which must have been present) allow the planets to effectively incorporate distant planetesimals into their envelope while still ejecting enough material to supply the Oort cloud. Our model's chief drawback is that we are not self-consistently treating the mass transfer in the outer Solar System; the mass moved outward will cause planetary orbital re-distribution in the system (Fernandez & Ip, 1984). Self consistently performing the 100-Myr simulations of planetesimal clearing was beyond the scope of this work. For Jupiter and Saturn, the amount of material ($\sim 10\%$ of the planet mass) is insufficient to move the planets very far, and thus we do not believe this will have much effect on the conclusion that their disks efficiently feed on the planetesimals within a few AU of their locations. For Uranus and Neptune the situation is less clear: (1) their migration scale may be longer than their protosatellite disks survive, (2) their small disk masses are not efficient planetesimal traps unless the planetesimals are very small, and (3) since they dominantly capture only local planetesimals, it is not clear that their locations matter very much. In summary, the gravitational 'clear out' of the planetesimals between the planets provide a natural mechanism to enrich the envelopes of Jupiter and Saturn to the observed extent.

Alibert et al.'s (2005) models differ by keeping the planetesimals non-dynamic but move Jupiter and Saturn to the low relative-velocity planetesimals (so that accretion cross-sections are high). The postulated migration sweeps the planets over many AU, and thus has a similar net enrichment effect. Our results show that the migration is not necessary since the planetesimals naturally come to, and are accreted by, the gas giants once they acquire their massive envelopes. Since plausible disks for plausible time scales around Jupiter and Saturn provide the cross-section, we can say that the large-scale migration is not required, even if some migration may have occurred.

Gaseous protosatellite disks provide a simple mechanism for enhancing the gas giants' capture cross-section while keeping the number of parameters relatively low (when compared to the more complex models). Although

the simplest case involving the concurrent formation of gas giant envelopes and disks is capable of reproducing the observed results, we point out that a delay between the onset of runaway gas accretion of Jupiter and Saturn may produce even more consistent results. Although the length of such a delay is largely unconstrained, this is an intriguing result. We find that taking estimated values from the literature, the heavy-element enrichments of the gas giants can be reproduced when the capture ability of the protosatellite disks are incorporated, in the physical setting of simultaneous planet formation, a delayed Saturn formation, or even an initially-compact giant-planet system.

Bibliography

- Alibert, Y., Mordasini, C., Benz, W., & Winisdoerffer, C., 2005, *Astronomy & Astrophysics* 434, 343
- Allende Prieto, C., Lambert, D. L., & Asplund, M., 2002, *Ap.J. (Letters)* 573, L137
- Anderson, J. D., Jacobson, R. A., McElrath, T. P., Moore, W. B., Schubert, G., & Thomas, P. C., 2001, *Icarus* 153, 157
- Atreya, S. K., Wong, M. H., Owen, T. C., Mahaffy, P. R., Niemann, H. B., de Pater, I., Drossart, P., & Encrenaz, T., 1999, *PlanSS* 47, 1243
- Barr, A. C. & Canup, R. M., 2008, in *Lunar and Planetary Institute Conference Abstracts*, Vol. 39 of *Lunar and Planetary Inst. Technical Report*, p. 2201
- Boss, A. P., 1997, *Science* 276, 1836
- Canup, R. M. & Ward, W. R., 2006, *Nature* 441, 834
- Chabrier, G. & Küker, M., 2006, *Astronomy & Astrophysics* 446, 1027
- Duncan, M. J. & Levison, H. F., 1997, *Science* 276, 1670
- Fernandez, J. A. & Ip, W.-H., 1984, *Icarus* 58, 109
- Franklin, F., Lecar, M., & Soper, P., 1989, *Icarus* 79, 223
- Fraser, W. C., Kavelaars, J. J., Holman, M. J., Pritchett, C. J., Gladman, B. J., Grav, T., Jones, R. L., Macwilliams, J., & Petit, J.-M., 2008, *Icarus* 195, 827
- Gladman, B. & Duncan, M., 1990, *A.J.* 100, 1680
- Gomes, R., Levison, H. F., Tsiganis, K., & Morbidelli, A., 2005, *Nature* 435, 466

- Guillot, T., 1999a, *PlanSS* 47, 1183
- Guillot, T., 1999b, *Science* 286, 72
- Guillot, T., 2005, *Annual Review of Earth and Planetary Sciences* 33, 493
- Guillot, T. & Gladman, B., 2000, in G. Garzón, C. Eiroa, D. de Winter, & T. J. Mahoney (eds.), *Disks, Planetesimals, and Planets*, Vol. 219 of *Astronomical Society of the Pacific Conference Series*, p. 475
- Hahn, J. M. & Malhotra, R., 1999, *A.J.* 117, 3041
- Haisch, Jr., K. E., Lada, E. A., & Lada, C. J., 2001, *Ap.J. (Letters)* 553, L153
- Helled, R., Podolak, M., & Kovetz, A., 2006, *Icarus* 185, 64
- Hubbard, W. B., Guillot, T., Marley, M. S., Burrows, A., Lunine, J. I., & Saumon, D. S., 1999, *PlanSS* 47, 1175
- Jayawardhana, R., Coffey, J., Scholz, A., Brandeker, A., & van Kerkwijk, M. H., 2006, *Ap.J.* 648, 1206
- Levison, H. F. & Duncan, M. J., 1993, *Ap.J. (Letters)* 406, L35
- Lissauer, J. J., 1993, *ARA&A* 31, 129
- Lodders, K., 2003, *Ap.J.* 591, 1220
- McKinnon, W. B., 2006, *LPI Contributions* 1335, 66
- Morbidelli, A., Levison, H. F., Tsiganis, K., & Gomes, R., 2005, *Nature* 435, 462
- Mosqueira, I. & Estrada, P. R., 2003, *Icarus* 163, 198
- Niemann, H. B., Harpold, D. N., Atreya, S. K., Carignan, G. R., Hunten, D. M., & Owen, T. C., 1992, *Space Science Reviews* 60, 111
- Owen, T., Mahaffy, P., Niemann, H. B., Atreya, S., Donahue, T., Bar-Nun, A., & de Pater, I., 1999, *Nature* 402, 269
- Pollack, J. B., Hubickyj, O., Bodenheimer, P., Lissauer, J. J., Podolak, M., & Greenzweig, Y., 1996, *Icarus* 124, 62
- Safronov, V. S. & Zvjagina, E. V., 1969, *Icarus* 10, 109

Bibliography

Trujillo, C. A., Jewitt, D. C., & Luu, J. X., 2000, *Ap.J. (Letters)* 529, L103

Tsiganis, K., Gomes, R., Morbidelli, A., & Levison, H. F., 2005, *Nature* 435, 459

Yoder, C. F., 1995, in T. J. Ahrens (ed.), *Global Earth Physics: A Handbook of Physical Constants*, p. 1

Appendix A

Consistency and Accuracy Tests

A.1 Core Mass

We assume that the giant planets formed quickly, and therefore begin the simulations of the baseline case with all planets possessing their current masses and radii. We also assume, however, that the planetesimals in the protoplanetary disk remain on circular orbits during this initial period of planet build-up. In order to verify the compatibility of these two assumptions, we investigated the orbital instability time scale between the planets while they are still present only as cores. We placed disk-less cores at the locations of Jupiter and Saturn, and distributed massless test particles from 6 to 8.5 AU. At the end of the 10 Myr simulation, we analyzed the the distribution of the particles to determine if they had been appreciably perturbed from their original orbits. We conducted such simulations for a variety of core masses ($1 - 90 M_{\oplus}$), and the results of the $10 M_{\oplus}$ cores simulation are shown in Figure A.1. This demonstrates that while the inclinations of the particles may be raised slightly in the course of 10 Myr, the majority of the particles remain in the same semimajor axis range. Furthermore, the snapshot of the particles' orbital elements was taken at 10 Myr, considerably longer than the planets are expected to remain as cores. This analysis therefore demonstrates that the orbital instability time scale between the planets exceeds the $\sim 1 - 3$ Myr expected time scale for dissipation of the the protosolar disk.

A.2 Eccentricity

Under the assumption that small planetesimals would not have been appreciably perturbed from circular heliocentric orbits by the fast formation of the giant planets, we set the initial eccentricity of all test particles to be 0. To test the validity of this assumption, we also ran a simulation in which the

initial planetesimal eccentricity was increased to 0.1. This simulation ran for the same duration and involved a comparable number of test particles. Using the same analysis techniques described for the preceding cases, it was apparent that the increased eccentricity cause less than a 10% effect on the final heavy element abundance of the giant planets. See table A.1.

Planet	Metallicity for $e_0 = 0$ (M_{\oplus})	Metallicity for $e_0=0.1$ (M_{\oplus})
Jupiter	18.5	21.3
Saturn	6.40	6.69
Uranus	4.10	4.37
Neptune	5.08	5.29

Table A.1: The final metallicities of the giant planets is comparable for the baseline ($e_0=0$) case and the case for which the planetesimals are assigned $e_0=0.1$. This demonstrates that our results are not sensitive to the initial eccentricity of the planetesimals if it remains low (in the neighbourhood of 0.1), and our assumption of an initially circular protoplanetary disk is therefore acceptable.

A.3 Close Encounter Log and Integration Step Size

Every time a test particle came within 0.1 AU of a planet (henceforth referred to as a ‘close encounter’), the planetocentric pericenter distance, test particle and planet Cartesian coordinates are logged. The pericenter distance is logged instantaneously, while the Cartesian orbital coordinates are logged at the next step interval. As we use the Cartesian coordinates to analyze the planetocentric orbit of the close encounter, it was necessary to ensure that the integration time step of 0.25 yr was sufficiently small to ensure accurate parameters. Comparing the logged pericenter to that calculated using the Cartesian coordinates provides an estimate of the error that recording only during the integration step introduces to the calculated orbit. As shown in Figure A.2, the logged and calculated pericenters are very close, differing by at most $\sim 10^{-6}$ AU for close encounters of planetesimals located within 0.014 AU ($30 R_{Jup}$) at the time of dump. This demonstrates that our step size is adequately small to ensure accurate recorded Cartesian coordinates.

A.4 Inclination distribution

Each time a particle passes through a planetary disk, the planetocentric orbital elements are calculated, allowing us to study both the individual close encounter and the properties of the distribution of orbits. The test particles are expected to have initial planetocentric orbits distributed roughly isotropically in inclination, and we are easily able to check the correspondence of the actual distribution to this expectation. The histogram of the inclination distribution for the planetesimal-jovian disk encounters in the baseline case (see Fig. A.3) is represented well by a $\sin(i)$ distribution to first order. The peak at 90° is understood as being due to having the most area available on the unit sphere for randomly oriented orbital poles.

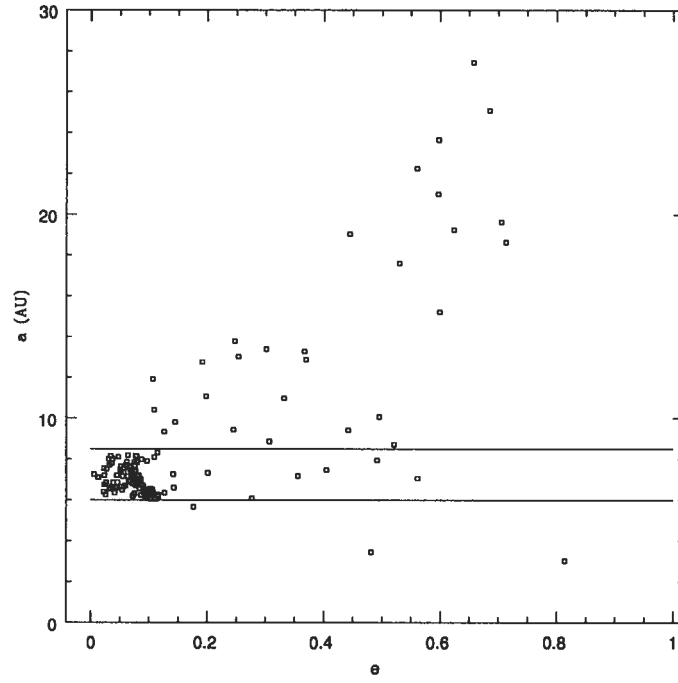


Figure A.1: The orbital elements at 10 Myr of planetesimals initially distributed between 6 to 8.5 AU (marked by horizontal lines) with eccentricity = 0. Both Jupiter and Saturn are given $10 M_{\oplus}$ cores for the duration of the simulation, and are located at 5.2 and 9.6 AU.

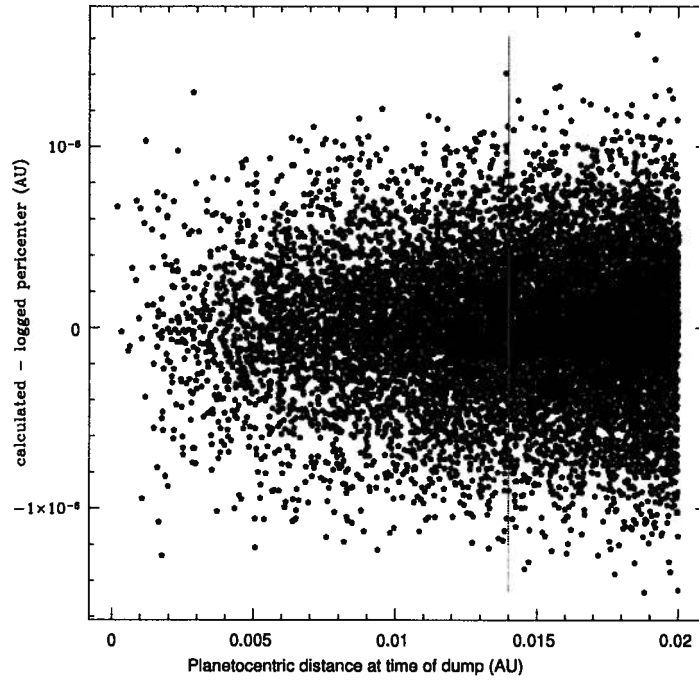


Figure A.2: Instantaneously logged pericenters compared to those calculated via the Cartesian coordinates recorded at the end of the step interval for the 150 Myr baseline case. Vertical line corresponds to $30 R_{Jup}$, the outer boundary of the disk. The negligible difference between values demonstrates the validity of using the logged Cartesian coordinates to ascertain orbital characteristics of flyby.

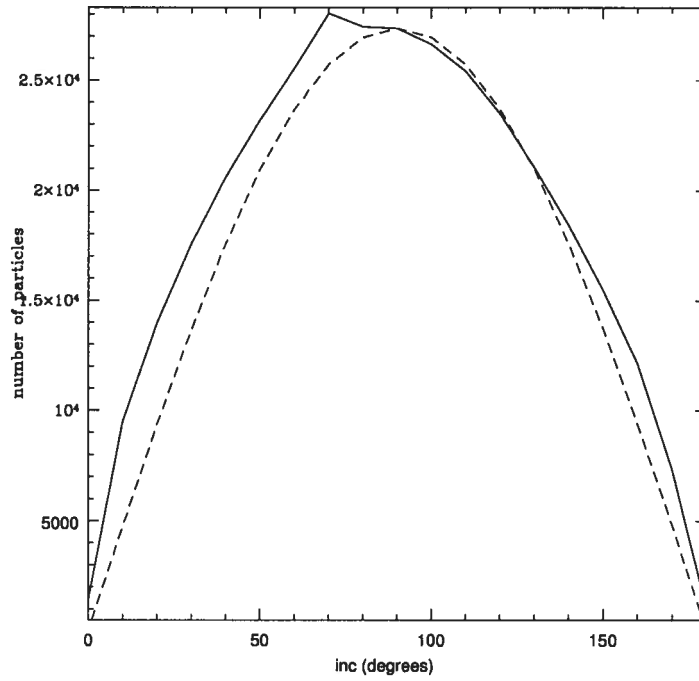


Figure A.3: The inclination distribution is characteristic of an isotropic population. The dotted curve, with functional form $N=27360*\sin(i)$, is simply to guide the eye and illustrate the conclusion that to first order the flybys arrive isotropically.

Appendix B

Notes on Publication

- Identification and design of research program: The main project was suggested by Dr. Brett Gladman. The specifics of the research program were decided upon by both Jaime Coffey and Dr. Gladman, and incorporated suggestions made by Dr. Tristan Guillot.
- Performing the research: The coding and running of the simulations was done by Jaime Coffey.
- Data analyses: The data was principally analyzed by Jaime Coffey. Suggestions were made principally by Dr. Gladman, with additional suggestions made by Dr. Guillot.
- Manuscript preparation: A portion of this thesis has been submitted to the *Astronomical Journal* for publication. Therefore, while the majority of the thesis was written by Jaime Coffey, Dr. Brett Gladman is the main author of portions of Section 2.0.1 as well as the entirety of Section 3.2.5. Figures 1.1 and 3.5 were constructed by Dr. Tristan Guillot